DOI: 10.1002/ejic.201000708

Low-Nuclearity Mn^{II} Complexes Based on Pyrimidine-4,6-dicarboxylato Bridging Ligand: Crystal Structure, Ion Exchange and Magnetic Properties

Garikoitz Beobide,[a,b] Oscar Castillo,*[a] Javier Cepeda,[a] Antonio Luque,*[a]
Sonia Pérez-Yáñez,[a] Pascual Román,[a] and Daniel Vallejo-Sánchez[a]

Keywords: Crystal engineering / Manganese / Ion exchange / Magnetic properties

The use of 1,10-phenanthroline (phen) has allowed the polymerisation process commonly occurring in manganese(II)/pyrimidine-4,6-dicarboxylate (pmdc) systems to be blocked off giving the first examples of low-nuclearity coordination compounds containing the pmdc dianion, namely, the dimeric $[Mn_2(\mu\text{-pmdc})_2(H_2O)_2(phen)_2]\cdot 8H_2O$ compound (**1**) and the tetrameric $[Mn_4(\mu\text{-pmdc})_3(phen)_4(H_2O)_4](X)_2\cdot 11H_2O$ [X = BF_4^- (**2**), ClO_4^- (**3**), NO_3^- (**4**)] complexes. X-ray analyses show that the hexacoordinate Mn^{II} atoms are bridged by pmdc dianions that exhibit an asymmetric $\kappa^2 N,O{:}\kappa O'$ coordination mode in compound **1** and adopt a bis-bidentate $\kappa^2 N,O{:}\kappa^2 N',O'$ binding pattern in the tetrameric units of compounds **2**–**4**. The distorted octahedral O_3N_3 donor set of the metal centres in **1** is completed by two nitrogen atoms from a phenanthroline ligand and one water molecule. In the linear zigzag shaped tetrameric cations of compounds **2**–**4**, the two inner manganese centres with a O_2N_4 donor set are, in addition, coordinated to two nitrogen atoms from a phenanthroline ligand, whereas the outer ones complete their O_3N_3 coordination environment with a bidentated phenanthroline ligand and two *cis* coordinated water molecules. The crystal packing of the complex units generates voids filled by hydrogen-bonded C3-like water chains in compound **1**, whereas compounds **2**–**4** resemble a 3D open-framework in which the channels are occupied by the counterions and the water molecules of crystallisation. Ion exchange tests were carried out showing that compound **4** exhibits a high capacity to capture other inorganic anions by releasing nitrates. Cryomagnetic susceptibility measurements have shown the occurrence of weak antiferromagnetic interactions (J = –0.06, –0.21, –0.26 and –0.25 cm^{-1} for compounds **1**–**4**, respectively). The magneto-structural analysis indicates that the magnetic interaction taking place through the μ-pyrimidine ring, although being weak, predominates over the longer exchange pathway involving the two carboxylate groups of the pmdc ligand.

Introduction

In the synthesis of solid networks from prefabricated molecular or ionic building blocks, that is, crystal engineering,[1] two omnipresent challenges are the ability to accurately design an infinite assembly based on structures of molecular building blocks and the ability to generate permanent pores in the material.[2] Central to the success of this field has been the creative utilisation and manipulation of hydrogen-bonding interactions[3] and coordination-driven assembly,[4] among other intermolecular forces.[5] The combination of these two tools is particularly powerful for constructing novel supramolecular species, for instance, using molecular metal clusters as building blocks.[6]

In this context, π-conjugated N-donor bridging ligands, such as diazines and their polycarboxylic derivatives, have appeared to be well-suited tools for the construction of coordinative bond-based extended arrays of metal ions with interesting physical properties in molecular magnetism or selective guest adsorption fields.[7,8] The carboxylation in the 4 and 6 positions of the pyrimidinic ring avoids the steric hindrance between the carboxylate groups and confers a planar topology to the dianion. This structural feature provides the pmdc with the potential capability to behave as a tetradentate bis-chelating ligand. In this regard, we have very recently reported a series of 1D coordination polymers of formula $\{[M(\mu\text{-pmdc})(H_2O)_2]\cdot H_2O\}_n$ (M = Fe, Co, Ni, Cu, Zn) and a 3D porous $\{[Mn(\mu\text{-pmdc})]\cdot 2H_2O\}_n$ compound, obtained by a self-assembly process involving divalent first row transition metal ions and the symmetric pyrimidine-4,6-dicarboxylate dianion.[9]

In this work, we couple the bridging capability of the pmdc ligand and the plasticity of the manganese(II) coordination sphere together with the presence of the blocking phenanthroline ligand to provide a variety of discrete entities that later assemble together by means of hydrogen bonding, aromatic π-π and electrostatic interactions. We also exploited the crystal structure directing effect that can

---

[a] Departamento de Química Inorgánica, Facultad de Ciencia y Tecnología, Universidad del País Vasco,
Apartado 644, 48080 Bilbao, Spain
Fax: +34-94601-3500
E-mail: oscar.castillo@ehu.es
antonio.luque@ehu.es
[b] Departamento de Procesos de Fabricación, Fundación Tekniker,
Avda Otaola 20, 20600 Eibar, Spain

Supporting information for this article is available on the WWW under http://dx.doi.org/10.1002/ejic.201000708.

exert the presence of counterions on the reaction media, and the ion exchange properties of some of these compounds have been evaluated.

Results and Discussion

The common structural feature of these compounds is the presence of the blocking phenanthroline ligand that affords discrete polynuclear entities in which the metal centres are bridged by pmdc ligands. The synthetic conditions, in particular the presence of high concentrations of different counterions, give rise to two different polynuclear entities.

[$Mn_2(\mu\text{-pmdc})_2(H_2O)_2(phen)_2$]·$8H_2O$ (1)

Compound **1** crystallises in the $P\bar{1}$ space group and its crystal structure consists of water molecules of crystallisation and centrosymmetric dinuclear complexes (Figure 1). The metal atoms are bridged by means of two pmdc ligands in a κ^2*O*,*N*:κ*O′* coordination mode, which leads to a five membered chelate ring around each metal with a chelating angle of 71.7°. As a consequence, the second carboxylate group is twisted 55.8° with respect to the diazine ring but the chelating carboxylate group is almost coplanar to it (9.6°). It is worth mentioning that such a coordination pattern has not been described until now in any pmdc complex. This double bridge establishes a M···M distance of 7.153 Å. The O_3N_3 coordination environment around the metal centres resembles a distorted octahedron and it is formed by a water molecule, two N atoms of a phen ligand, the chelating N and O atoms of one of the pmdc ligands, and one O-carboxylate atom of the second pmdc ligand. The coordinate bond lengths (Table 1) involving the O atoms are slightly smaller than those corresponding to N atoms with average values of 2.14 and 2.28 Å for Mn–O and Mn–N, respectively.

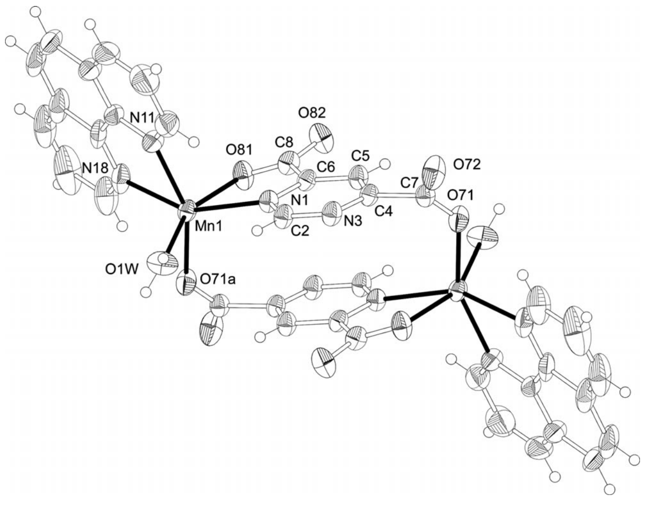

Figure 1. ORTEP view of the dinuclear entity of compound **1** showing the labelling scheme.

Table 1. Selected bond lengths [Å] for the coordination polyhedra of compounds **1**–**3**.[a]

	1		2	3
Mn1–N1	2.352(3)	Mn1–N12	2.246(4)	2.260(3)
Mn1–O81	2.157(3)	Mn1–O151	2.180(3)	2.179(3)
Mn1–O71a	2.157(3)	Mn1–N21	2.295(4)	2.294(3)
Mn1–N11	2.254(4)	Mn1–O281	2.156(3)	2.160(3)
Mn1–N18	2.248(4)	Mn1–N31	2.253(4)	2.257(4)
Mn1–O1w	2.117(3)	Mn1–N38	2.220(4)	2.223(4)
		Mn2–N23	2.335(4)	2.345(3)
		Mn2–O271	2.136(4)	2.143(3)
		Mn2–N51	2.229(5)	2.231(4)
		Mn2–N58	2.262(5)	2.286(4)
		Mn2–O1w	2.152(4)	2.154(3)
		Mn2–O2w	2.123(4)	2.140(3)

[a] Symmetry code, a: – *x* + 2, –*y*, –*z* + 1.

The dinuclear entities are linked together by means of π-π stacking interactions among the phen ligands and by hydrogen bonds involving the O1w atom of the coordinated water molecule and the noncoordinated O82 atom of the chelating carboxylate group to generate layers parallel to the crystallographic *ac* plane (Figure 2). One-dimensional chains of hydrogen-bonded water molecules of crystallisation that run along the crystallographic *a* axis are placed in the interlamellar space (ca. 20 % of the total volume of the unit cell). The most frequent pattern of water chains consists of repeating units of four molecules [C4].[10] The water chain observed in compound **1**, however, resembles a C3 (O3w, O4w, O5w) pattern with an additional water molecule (O2w) attached to the main chain through a single hydrogen bond. These water clusters act as interlamellar double adhesive tapes bridging complexes from upper and lower layers by means of an extensive network of hydrogen bonds (see the Supporting Information).

[$Mn_4(\mu\text{-pmdc})_3(phen)_4(H_2O)_4$]$(X)_2$·$11H_2O$ [X = BF_4^- (2), ClO_4^- (3), NO_3^- (4)]

Compounds **2**–**4** are isostructural and are built up of water molecules of crystallisation, inorganic anions (BF_4^-/ClO_4^-/NO_3^-) and axiosymmetric tetranuclear cationic complexes, in which metal centres are bridged by bis-bidentate pmdc ligands in a zigzag arrangement (Figure 3, a). The asymmetric unit of the tetranuclear moiety (Figure 3, b) consists of two Mn^{II} atoms (Mn1, Mn2), two phen ligands (phen-1, phen-2), two water molecules (O1w, O2w) and one and half pmdc ligand (pmdc-1, pmdc-2). Pmdc-1 is cut off along by a binary axis (C11···C14), which generates the remaining part of the complex. The main bond lengths around the metal centres are given in Table 1. The O_2N_4 donor set of the inner metal atoms (Mn1) resembles a distorted octahedron formed by four nitrogen atoms and two oxygen atoms in *trans* position from three chelating ligands (phen-1, pmdc-1 and pmdc-2). The outer metal centres (Mn2) show an O_3N_3 chromophore that consists of two N atoms from the blocking phen-2 ligand, one N atom and one O atom from the pmdc-2 bridge, and two *cis*-coordinated water molecules.

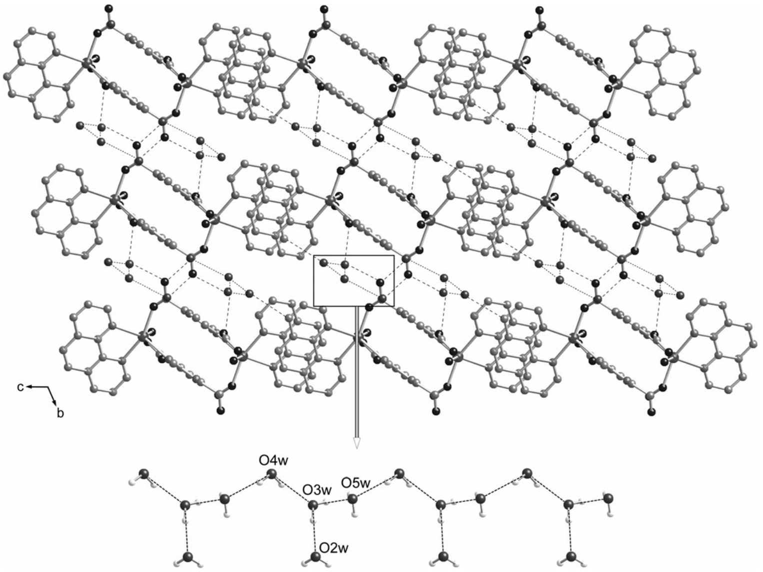

Figure 2. Crystal packing of compound **1** viewed along the crystallographic *a* axis (top) and the hydrogen-bonded chain of water molecules (bottom).

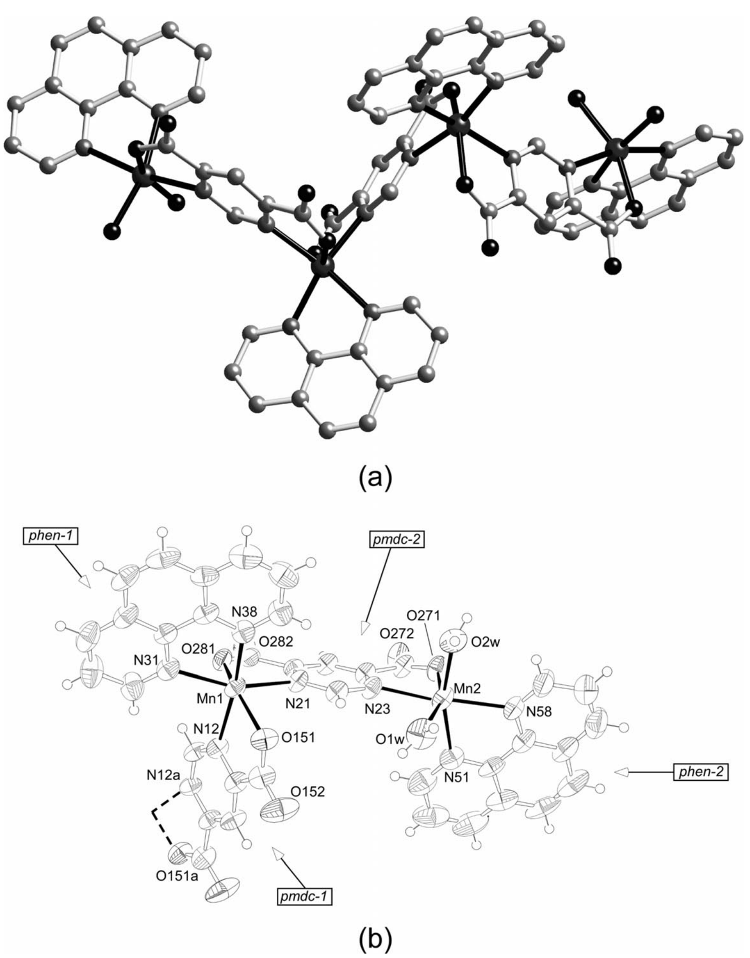

(a)

(b)

Figure 3. (a) Perspective view of the tetranuclear cation of compounds **2** and **3**. (b) ORTEP drawing of the corresponding asymmetric unit.

The chelate rings established by the pmdc ligands display bite angles ranging from 72.3 to 73.2°. The deviation of the Mn1 atom from the mean plane of the pyrimidine ring of pmdc-1 (0.266 and 0.300 Å for compounds **2** and **3**, respectively) is considerably greater than that corresponding to pmdc-2 (0.059 and 0.037 Å), whereas the deviation of the

Mn2 atom from the diazine ring of pmdc-2 presents an intermediate value (0.096 and 0.122 Å). Pmdc-1 is almost planar with a dihedral angle among the carboxylate groups and the diazine ring of 3.1 and 3.8° for compounds **2** and **3**, respectively. One of the carboxylate groups of pmdc-2 is almost coplanar to the diazine ring (3.7 and 5.7°), whereas the second one is significantly twisted (12.2 and 12.6°, respectively). The M···M distances through pmdc-1 (6.412 and 6.450 Å for compound **2** and **3**, respectively) are slightly smaller than those corresponding to pmdc-2 (6.648 and 6.673 Å).

The tetrameric entity exhibits some similarities with the zigzag 1D chains found in the previously reported $\{[Mn(\mu\text{-pmdc})(H_2O)_3]\cdot 2H_2O\}_n$ and $\{[Mn_2(\mu\text{-pmdc})_2(H_2O)_5]\cdot 2H_2O\}_n$ compounds.[9a] The corrugation degree of these chains is related to the M···M···M angle and the dihedral angle between two neighbouring bridges. The M···M···M angles within the tetrameric Mn^{II} complex are 109.1 and 108.9° for compounds **2** and **3**, respectively, whereas the dihedral angles between two successive bridging ligands are 85.5 and 84.5°. The zigzag polymeric Mn^{II}–pmdc complexes show a more corrugated conformation with remarkably smaller angles (M···M···M: 63.2–71.2°; pmdc/pmdc: 58.2–74.1°) due to the greater steric hindrance that exerts the hepta-coordination around the metal centres. The tetrameric units and polymeric Mn^{II} chains both have the presence of pmdc bridges and their donor N atoms in *cis* position, which promote a zigzag arrangement. When the N-pmdc atoms are in *trans* position, however, linear or slightly corrugated chains are generated depending on the *trans*- or

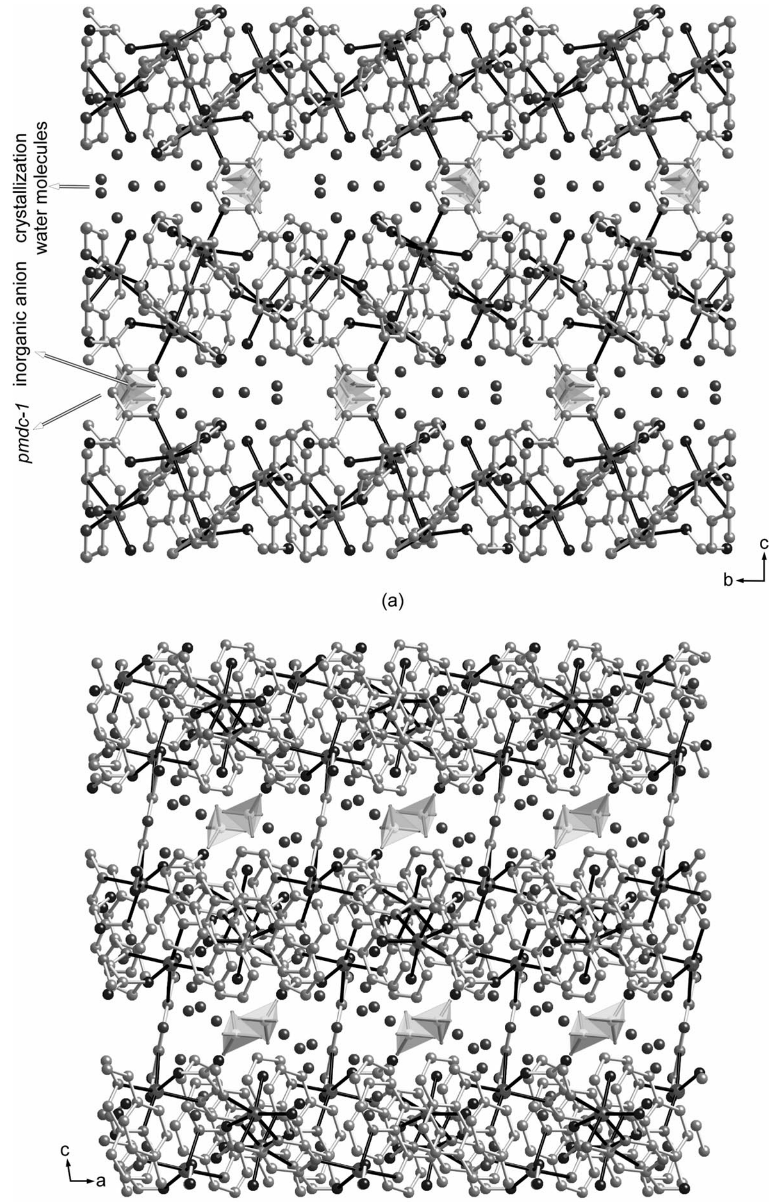

(a)

(b)

Figure 4. Views of the crystal packing of compound **2**.

cis-positioning of the O-pmdc atoms. Examples of these two dispositions are evident in the compounds {[M(μ-pmdc)$(H_2O)_2$]·H_2O}$_n$ [linear chain: N/O-pmdc in *trans*/*trans* position: M···M···M: 177–180°; pmdc/pmdc: 0.0–10.6°] and {[Cu(μ-pmdc)(dpa)]·$4H_2O$}$_n$ [corrugated chain: N/O-pmdc in *trans*/*cis* positions: M···M···M: 170.7°; pmdc/pmdc: 81.0°].[9b]

The crystal buildings of compounds **2** and **3** can be described as a pillared lamellar structure in which each tetrameric cation is divided into two fragments linked through a pmdc-1 pillar ligand (Figure 4). Within each layer, the fragments of metal complexes are cross-linked by means of the hydrogen-bonding interactions established between the coordinated O1w and O2w water molecules and the non-coordinated O152 and O282 carboxylate atoms, leading to a row-like arrangement (Figure 5).

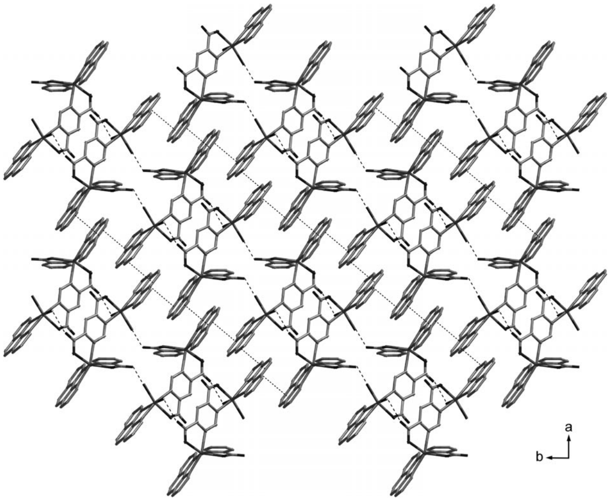

Figure 5. Layers of fragments of the tetranuclear complexes sustained by π–π interactions (dotted lines) and hydrogen bonds (dashed lines) in compound **2**.

Additionally, these rows assemble as a zipper-like structure sustained by means of offset face-to-face π–π interactions between the aromatic rings of the phen-1 and phen-2 ligands (see the Supporting Information). The arrangement of the cationic complexes generates channels along the crystallographic [100] and [010] directions in which the solvation water molecules and the inorganic anions are accommodated. The potentially available volume occupied by the water molecules of crystallisation represents 16% of the total volume of the unit cell, whereas that filled by both the inorganic anions and crystallisation water rises to 27%. This supramolecular network confers a certain degree of flexibility into the crystal lattice of these compounds, which is evidenced by the slight lengthening of the c parameter when the more voluminous perchlorate anion (**3**) substitutes tetrafluoroborate anion (**2**) (Δc: 0.167 Å, ΔV: 23 Å^3).

To gain further insight into the robustness of the supramolecular crystal buildings, thermogravimetric and variable temperature X-ray powder diffraction studies were performed on compound **2**. The thermogravimetric measurement shows a first mass loss beginning at room temperature, which corresponds to the release of the crystallisation and coordinated water molecules (exp. 14.15%, calcd. 14.34%). This process is accompanied by the collapse of the crystal structure to give an amorphous anhydrous compound that remains stable from 130 to 270 °C. Upon heating above this temperature the compound suffers several exothermic processes leading to a mixture of $MnBO_3$ and Mn_2O_3 as the final residue at 620 °C (see the Supporting Information).

Ion Exchange

Many inorganic or metal-organic compounds with open frameworks have shown the capability of adsorbing neutral species, exchanging ions or catalysing reactions within the channels,[11] thereby having a broad range of potential applications. For instance, materials with ionic exchange capacity are very valuable to capture toxic or radioactive charged chemical species. With regard to this matter, it can be expected that the open and flexible structures of compounds **2**–**4** allow the transit of anionic species within the channels and therefore, the chance of exchange by similar chemical species.

To qualitatively verify this approach, two samples of compound **4** were exposed to aqueous solutions of either $NaBF_4$ or $NaClO_4$ at room temperature in a complex:salt molar ratio of 1:3. The evolution of the ion exchange process was monitored by sampling at different exposure times and collecting the FTIR spectra. The stretching band of outgoing nitrate anion sited at approximately 1385 cm^{-1} can be easily distinguished from those corresponding to the incoming tetrafluoridoborate (1030–1125 cm^{-1}) and perchlorate (1105–1120 cm^{-1}) anions. Figure 6 depicts the FTIR spectra collected before (t = 0 h) and after (t = 1 h and t = 8 h) exposure to the salt solution. As time passes, the band corresponding to the nitrate anion progressively decreases, whereas the band intensity of the tetrafluoridoborate and perchlorate anions increases. Finally, the absence of the characteristic band at 1385 cm^{-1} in the sample after 8 h indicates that NO_3^- has been almost quantitatively removed. Moreover, XRPD patterns and elemental analyses of the resulting compounds match those observed for the pure tetrafluoridoborate (**2**) and perchlorate (**3**) compounds. Therefore, the nitrate anion of compound **4** can be substituted while retaining the integrity of the host structure. No change has been observed in the IR spectra and XRPD patterns when additional amounts of nitrate salts are added to the same batch after the ion exchange process.

The experiment was repeated using compounds **2** and **3** as starting materials. Unfortunately, neither showed any significant degree of ionic exchange of the nitrate anion, and only when prolonged exposure times have been imposed, traces of a partial substitution are observed. This fact suggests that the nitrate anion is weakly bound to the host structure and it presents a greater mobility along the channels, whereas once tetrafluoridoborate or perchlorate are captured they anchor relatively tightly to the surrounding framework and as a consequence, they are hard to remove.

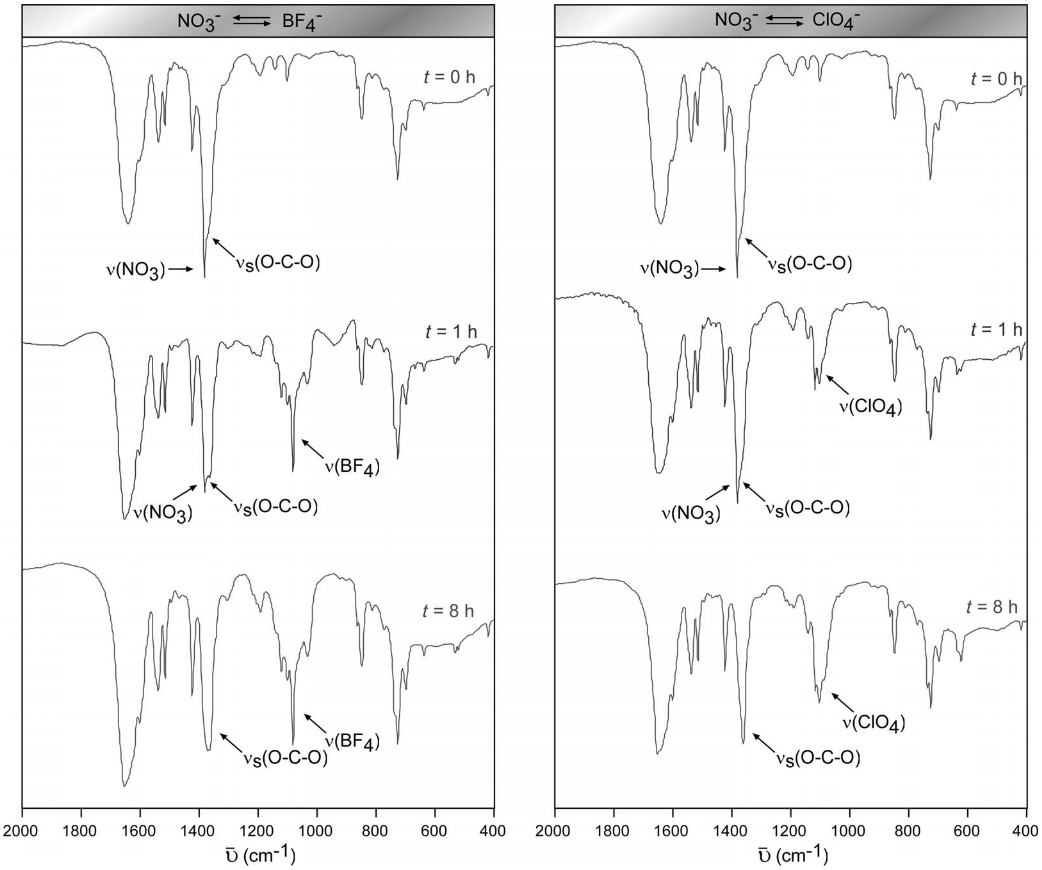

Figure 6. FTIR monitoring of the NO_3^-/BF_4^- (left) and NO_3^-/ClO_4^- (right) ion exchange processes in compound **4**.

The nature of the ion exchange could be attributed to both a solid-state diffusion and exchange mechanism or to a recrystallisation process mediated by the partial solubilisation of the starting material. To obtain additional information about the possible mechanism, a suspension of 60 mg of compound **4** in 25 mL of water was stirred over 48 h at 20 °C. The resulting suspension was filtered off and the manganese content in the mother liquid was found to be 63 ppm by ICP. This value only represents approximately 0.03% of the total starting amount of compound **4**. It seems to indicate that a solid-state diffusion and exchange process is the responsible for the ion exchange observed in these compounds.

Magnetic Properties

Compounds **1**–**4** show a room temperature $\chi_M T$ value close to that expected for a cluster of two (**1**) and four (**2**–**4**) uncoupled manganese(II) ions (Table 2). All of them show a continuous decrease of the $\chi_M T$ value with the lowering of the temperature (Figure 7), indicating an overall antiferromagnetic behaviour. In addition, the absence of any maximum in the χ_M curve suggests the weakness of the magnetic interactions. This behaviour agrees with the reported antiferromagnetic interactions for metal ions containing e_g unpaired electrons bridged by pyrimidine type ligands,[12] in contrast with the ferromagnetic behaviour usually observed for compounds containing only t_{2g} unpaired electrons.[13]

Table 2. Magnetic data of compounds **1**–**4**.[a]

	$\chi_M T$ (300 K) Exp.	Calcd.	J [cm^{-1}]	g	$R \cdot 10^4$
1	8.84	8.76	–0.06	2.00	0.7
2	17.92	17.52	–0.21	2.00	17.3
3	18.04	17.52	–0.26	2.00	10.7
4	18.01	17.52	–0.25	2.00	12.5

[a] $R = \Sigma_i[(\chi_M T)_{obsd.}(i) - (\chi_M T)_{calcd.}(i)]^2/\Sigma_i[(\chi_M T)_{obsd.}(i)]^2$.

Taking into account the molecular structure of compound **1**, its magnetic data have been fitted using the Bleaney–Bowers equation for a dinuclear entity derived from $H = -JS_1 \cdot S_2$.[14] In the case of compounds **2**–**4**, the magnetic data have been fitted to a linear tetramer by using MAGMUN4.1 software[15] and considering $H = -J(S_1 \cdot S_2 + S_2 \cdot S_3 + S_3 \cdot S_4)$ as spin Hamiltonian. The spin energy spectrum is calculated and inserted into the Van Vleck equation to carry out the subsequent fitting of the experimental data. The obtained J values for compounds **2**–**4** are similar to those found in Mn^{II} polymeric 1D complexes (ca. –0.2 cm^{-1}) in which the pmdc bridging ligand displays the same tetradentate $\kappa^2 O,N{:}\kappa^2 O',N'$ coordination mode.[9a] For this coordination pattern, the magnetic exchange takes

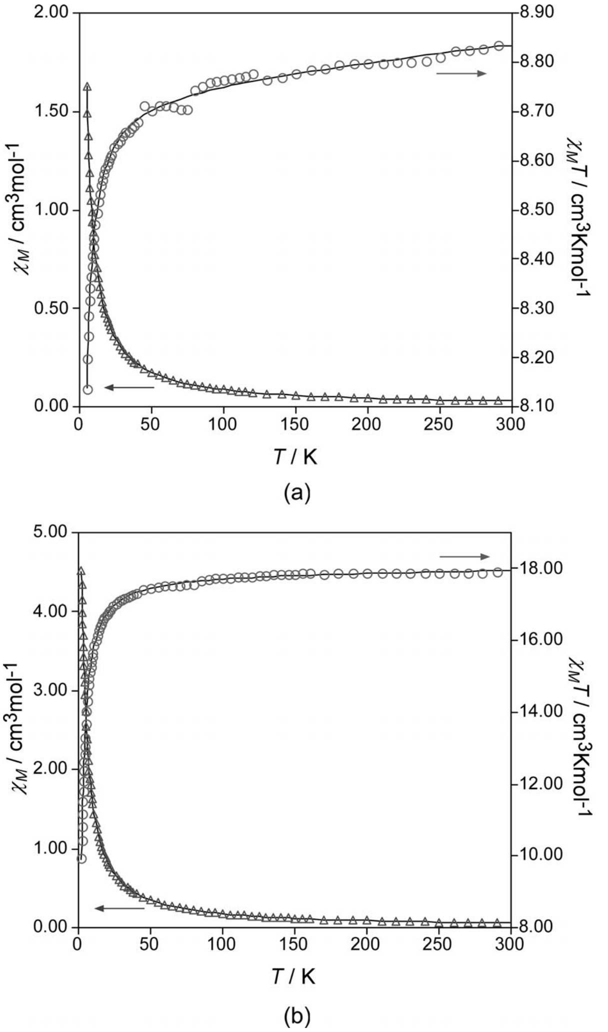

Figure 7. The thermal variation of the χ_M and $\chi_M T$ values at 5 kOe for (a) compound **1** and (b) compound **2**. Solid lines correspond to the line of best fit (see text).

place mainly along the diazine ring. In fact, the achieved *J* values are within the range reported for μ-pyrimidine-bridged Mn^{II} complexes (from –0.2 to –0.3 cm^{-1}).[16] This reasoning is in concordance with the low *J* value observed (–0.06 cm^{-1}) in compound **1**, in which the two Mn^{II} centres are connected through a double $O–C_{carb}\cdots N_{pym}$ pathway and thus, it can be inferred that a negligible interaction occurs through the carboxylate groups in all the aforementioned pmdc-bridged complexes.

Conclusion

As has been previously reported, transition metal ions (M^{2+}), such as manganese(II), tend to polymerise in the presence of the pyrimidine-4,6-dicarboxylate dianion leading to linear or corrugated 1D chains.[9] Such behaviour is directed by the preponderant bis-bidentate coordination mode of the pmdc bridge. Nonetheless, the control of the reaction conditions and stoichiometry can promote novel coordination modes and the formation of skeletons of greater nuclearity, as it has been proven in previously reported 2D and 3D Mn^{II} complexes.[9a,17] It deserves to note, that among all reported pmdc transition metal complexes, those with Mn^{II} as the metal centre present the greatest structural diversity. In this respect, the Mn^{II}-pmdc couple provides a useful system to develop novel intriguing structures. The complexes described herein are excellent examples of the versatile building capabilities of the Mn–pmdc couple. Moreover, they represent the first discrete complexes based on pyrimidine-4,6-dicarboxylate ligand. The use of 1,10-phenanthroline as blocking ligand stops the polymerisation process and allows the crystallisation of dinuclear neutral species when small anions are present in the synthetic mixture (Cl^-) by means of slow solvent evaporation. The addition of a bulkier anion (BF_4^-, ClO_4^-, NO_3^-), with several hydrogen bonding acceptor sites, however, promotes the immediate precipitation of tetranuclear complexes. The self-assembly of the tetranuclear units leads to open 3D frameworks with channels hosting water molecules and anions. The overall supramolecular structures show the capability of irreversibly capturing anions, such as BF_4^- and ClO_4^-, when the nitrate complex salt is employed as starting material.

Experimental Section

CAUTION: Perchlorate salts of metal complexes with organic ligands are potentially explosive and should be handled with care.

Reagents: All chemicals were of reagent grade and were used as commercially obtained. The starting material K_2pmdc was prepared following the previously reported procedure.[18]

Physical Measurements: Elemental analyses (C,H,N) were performed on a Euro EA (EuroVector) Elemental Analyzer. Metal content was determined by atomic absorption spectrometry (Perkin–Elmer Analyst 100). The IR spectra (KBr pellets) were recorded on a FTIR 8400S Shimadzu spectrometer in the 4000–400 cm^{-1} spectral region. Thermal analyses (TG/DTG/DTA) were performed on a TA Instruments SDT 2960 thermal analyzer in a synthetic air atmosphere (79 %N_2/21 %O_2) with heating rate of 5 °C·min^{-1}. Magnetic measurements were performed on polycrystalline samples of the compounds with a Quantum Design SQUID susceptometer covering the temperature range of 2.0–300 K at 0.5 T. The susceptibility data were corrected for the diamagnetism estimated from Pascal's tables,[19] the temperature-independent paramagnetism and the magnetisation of the sample holder.

Single-Crystal X-ray Data Collection and Structure Determination: Data collections on single crystals of compounds **1**–**3** were carried out at 293 K with an Xcalibur diffractometer equipped with an area detector and graphite-monochromated Mo-K_α radiation (λ = 0.71073 Å). The data reduction was done with the CrysAlis RED program.[20] Information concerning data collection is summarised in Table 3. The structures were solved by direct methods using the SIR97 program.[21] Full matrix least-squares refinements were performed on F^2 using SHELXL97.[22] All calculations were performed using the WinGX crystallographic software package.[23]

All non-hydrogen atoms were refined anisotropically, except those corresponding to the inorganic anions and the water molecules of crystallisation of compounds **2**–**3** due to the high degree of disorder. To simulate such disorder, the inorganic anion has been split

Table 3. Single-crystal X-ray data and structure refinement details for compounds **1**–**3** and unit cell parameters from XRPD data for compound **4**.

	1	**2**	**3**	**4**
Formula	$C_{36}H_{40}Mn_2N_8O_{18}$	$C_{66}H_{68}B_2F_8Mn_4N_{14}O_{27}$	$C_{66}H_{68}Cl_2Mn_4N_{14}O_{35}$	$C_{66}H_{68}Mn_4N_{16}O_{33}$
M_r	982.64	1882.69	1907.98	1833.09
Crystal system	triclinic	monoclinic	monoclinic	monoclinic
Space group	$P\bar{1}$	$C2/c$	$C2/c$	$C2/c$
a [Å]	7.620(1)	17.304(1)	17.282(1)	17.303(4)
b [Å]	9.643(2)	21.851(1)	21.744(2)	21.818(4)
c [Å]	14.701(3)	20.636(2)	20.803(2)	20.721(5)
α [°]	99.56(2)	90(–)	90(–)	90(–)
β [°]	98.39(2)	94.333(5)	93.445(7)	93.93(2)
γ [°]	102.48(2)	90(–)	90(–)	90(–)
V [Å^3]	1021.3(4)	7780(1)	7803(1)	7804(3)
Z	1	4	4	4
$\rho_{calcd.}$ [g cm^{-3}]	1.598	1.615	1.624	
μ [mm^{-1}]	0.707	0.743	0.804	
Unique data/parameters	8983/290	8721/526	9490/516	
Reflections with $I \geq 2\sigma(I)$	6512	3135	3000	
$R1^{[a]}/wR2^{[b]}$ [$I \geq 2\sigma(I)$]	0.0848/0.2515	0.0659/0.1704	0.0592/0.1468	
$R1/wR2$ (all data)	0.1051/0.2705	0.1648/0.2000	0.1566/0.1593	

[a] $R_1 = \Sigma||F_o| - |F_c||/\Sigma|F_o|$. [b] $wR_2 = [\Sigma w(F_o^2 - F_c^2)^2/\Sigma wF_o^2]^{1/2}$; $w = 1/[\sigma^2(F_o^2) + (aP)^2]$ where $P = [\max(F_o^2,0) + 2F_c^2]/3$ with a = 0. 2000 (for **1**), 0.1137 (for **2**) and 0.0835 (for **3**).

into two rigid fragments refining their positions and occupation factors. In the case of the water molecules of crystallisation, the high degree of disorder did not allow the hydrogen atoms to be located and half occupation factors have been applied to some of them to reproduce the disorder present in these compounds.

Compound **1** crystallises as a non-merohedral twin, in which both parts of the twin are related by means of a binary rotation axis along the [001] direction (twin law: –1 0 0/0 –1 0/0.736 0.632 1). Structure refinement was carried through SHELX97 using HKLF5 and BASF entries, which revealed a fractional value of 0.24 for the minor domain.

CCDC-782337 (for **1**), -782338 (for **2**) and -782339 (for **3**) contain the supplementary crystallographic data for this paper. These data can be obtained free of charge from The Cambridge Crystallographic Data Centre via www.ccdc.cam.ac.uk/data_request/cif.

X-ray Powder Diffraction Data Collection: X-ray powder diffraction data for polycrystalline samples of compound **4** were collected on a Phillips X'PERT powder diffractometer with Cu-K_α radiation in steps of 0.03° over the 2θ 10–70° range with a fixed-time counting of 20 s at 298 K. The resemblance between the experimental XRPD pattern of compound **4** and the simulated patterns of compounds **2**–**3** reveals that they are all isostructural (Figure 8). It must be mentioned that FTIR spectroscopy, elemental analysis and thermogravimetric measurements (see the Supporting Information) support this crystallographic relationship and they agree with the formula $[Mn_4(\mu\text{-pmdc})_3(phen)_4(H_2O)_4](NO_3)_2\cdot$ca.$11H_2O$. Minor differences among the XRPD patterns can be attributed to the substitution of the inorganic anion and to the low temperature release of some water molecules of crystallisation during the sample preparation, as it can be inferred from the thermogravimetric measurements (ca. 28 °C).

The low crystallinity of compound **4** did not allow an acceptable refinement of the whole crystal structure from XRPD data. Refinement of the diffraction pattern with the FULLPROF program[24] using the space group and cell parameters of compound **2** as starting data, however, lead to the cell parameters gathered in Table 3.

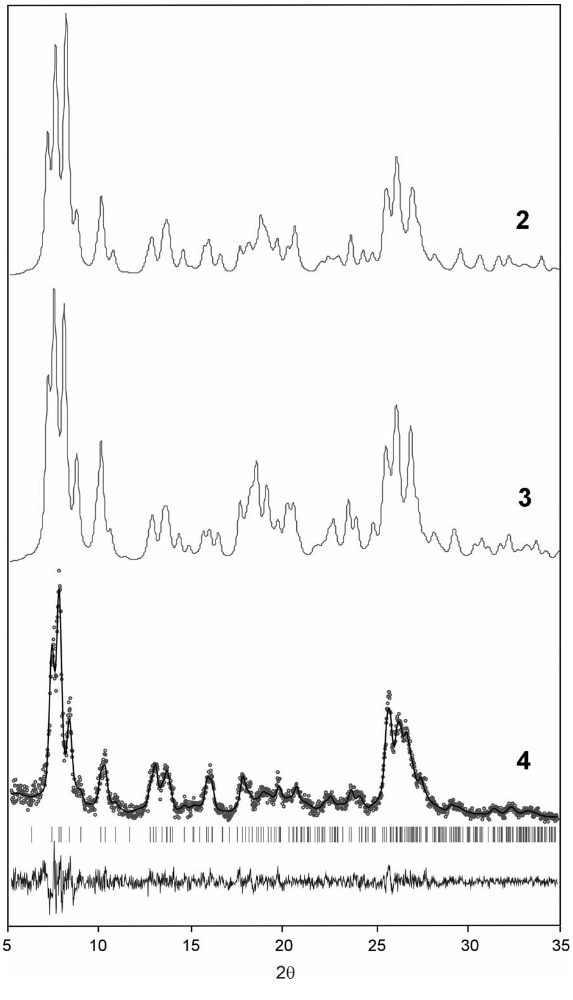

Figure 8. Simulated X-ray powder diffraction patterns for compounds **2** and **3** (FWHM = 0.5), together with the experimental (circles) and calculated (solid line) patterns for compound **4**.

[$Mn_2(\mu$-pmdc$)_2(H_2O)_2($phen$)_2]\cdot 8H_2O$ (1): An aqueous solution (10 mL) of K_2pmdc (0.0611 g, 0.50 mmol) was added dropwise to a methanol solution (10 mL) of $MnCl_2\cdot 2H_2O$ (0.0809 g, 0.50 mmol) and 1,10-phenanthroline (0.0901 g, 0.50 mmol). The resulting light-yellow solution was allowed to evaporate at room temperature. Two weeks later, light yellow single-crystals of **1** were obtained; yield 160 mg (65%). $C_{36}H_{40}Mn_2N_8O_{18}$ (982.64): calcd. C 44.00, H 4.10, N 11.40, Mn 11.18; found C 44.09, H 4.21, N 11.50, Mn 11.48. Main IR features (KBr pellet): $\tilde{\nu}$ = 3422 (vs), 3272 [sh vs, ν(O–H)], 3077 [w, ν(C–H)], 1648 [vs, ν_{as}(O–C–O)], 1543 (s), 1515 [s, ν(C=C, C=N)], 1475 [w, ν(C_{ar}–C)], 1427 (s), 1369 [vs, ν_s(O–C–O)], 1311 (w), 1182 (w), 1098 (w), 1049 [w, δ_{ip}(C–H)], 924 [w, δ_{op} (C–H)], 848 (m), 831 [sh, δ_{ring}], 728 [m, δ_{ip}(O–C–O)], 693 [w, δ_{op}(O–C–O)], 640 (w), 511 [w, τ_{ring}], 422 [w, ν(M–O, M–N)] cm^{-1}.

[$Mn_4(\mu$-pmdc$)_3($phen$)_4(H_2O)_4](X)_2\cdot 11H_2O$ [X = BF_4^- (2), ClO_4^- (3), NO_3^- (4)]: Compounds **2**–**4** were prepared analogously to **1**, but immediately after mixing K_2pmdc, $MnCl_2\cdot 2H_2O$ and 1,10-phenanthroline into an aqueous methanolic solution, an aqueous solution (5 mL) of $NaBF_4$ (0.0549 g, 0.50 mmol), $NaClO_4\cdot H_2O$ (0.0702 g, 0.50 mmol) or KNO_3 (0.0506 g, 0.50 mmol) was added dropwise. The resulting solution was stirred for few minutes until a yellowish precipitate corresponding to compounds **2**–**4** appeared. The recrystallisation of these polycrystalline powders from an aqueous-methanolic solution (3:2 v:v, 50 mL) allowed the growth of orange crystals of **2** and **3** suitable for X-ray diffraction analysis.

2: Yield 153 mg (65%). $C_{66}H_{68}B_2F_8Mn_4N_{14}O_{27}$ (1882.69): calcd. C 42.11, H 3.64, N 10.42, Mn 11.67; found C 42.19, H 3.52, N 10.50, Mn 11.65. Main IR features (KBr pellet): $\tilde{\nu}$ = 3427 [vs, ν(O–H)], 3061 [w, ν(C–H)], 1653 (vs), 1604 [m, ν_{as}(O–C–O)], 1538 (m), 1516 [m, ν(C=C, C=N)], 1471 [w, ν(C_{ar}–C)], 1427 (s), 1364 [vs, ν_s(O–C–O)], 1191 (w), 1102 [w, δ_{ip}(C–H)], 1124 (w), 1084 (s), 1031 [w, ν(BF_4)], 924 (w), 902 [w, δ_{op} (C–H)], 849 [m, δ_{ring}], 729 [m, δ_{ip}(O–C–O)], 698 [w, δ_{op}(O–C–O)], 636 [w, τ_{ring}], 413 [w, ν(M–O, M–N)] cm^{-1}.

3: Yield 167 mg (70%). $C_{66}H_{68}Cl_2Mn_4N_{14}O_{35}$ (1907.98): calcd. C 41.55, H 3.59, N 10.28, Mn 11.52; found C 41.60, H 3.49, N 10.35, Mn 11.58. Main IR features (KBr pellet): $\tilde{\nu}$ = 3428 [vs, ν(O–H)], 3061 [w, ν(C–H)], 1644 (vs), 1604 [sh, ν_{as}(O–C–O)], 1538 (m), 1516 [m, ν(C=C, C=N)], 1471 [w, ν(C_{ar}–C)], 1427 (s), 1369 [vs, ν_s(O–C–O)], 1191 (w), 1142 [w, δ_{ip}(C–H)], 1120 (s), 1107 [s,, ν(ClO_4)], 924 (w), 902 [w, δ_{op} (C–H)], 849 [m, δ_{ring}; 729 [m, δ_{ip}(O–C–O)], 698 [w, δ_{op}(O–C–O); 636 [w, τ_{ring}], 413 [w, ν(M–O, M–N)] cm^{-1}.

4: Yield 138 mg (60%). $C_{66}H_{68}Mn_4N_{16}O_{33}$ (1833.09): calcd. C 43.24, H 3.74, N 12.23, Mn 11.99; found C 43.34, H 3.51, N 12.32, Mn 12.05. Main IR features (KBr pellet): $\tilde{\nu}$ = 3422 [vs, ν(O–H)], 3061 [w, ν(C–H)], 1653 (vs), 1604 [sh, ν_{as}(O–C–O)], 1538 (m), 1515 [m, ν(C=C, C=N)], 1471 [w, ν(C_{ar}–C)], 1427 (s), 1368 [sh, ν_s(O–C–O)], 1387 [vs, ν(NO_3)], 1191 (w), 1138 (w), 1102 [w, δ_{ip}(C–H)], 924 (w), 902 [w, δ_{op}(C–H)], 849 [m, δ_{ring}], 729 [m, δ_{ip}(O–C–O)], 697 [w, δ_{op}(O–C–O)], 636 [w, τ_{ring}], 413 [w, ν(M–O, M–N)]cm^{-1}.

The addition to the synthesis media of compound **1** of an excess of chloride anions provides only this dimeric compound without any evidence of the presence of species analogous to those of compounds **2**–**4**, as checked by visual inspection and X-ray diffraction techniques.

Supporting Information (see also the footnote on the first page of this article): FTIR spectra of compounds **1**–**4**. Thermogravimetric data of compounds **1**, **2** and **4**. Variable-temperature diffraction pattern of compound **2**. Structural parameters of the coordination environments and the noncovalent interactions.

Acknowledgments

This work was supported by the Ministerio de Ciencia e Innovación (MCINN) (MAT2008-05690/MAT), the Gobierno Vasco (IT-477-10). J. C. and S. P.-Y. thank Universidad del País Vasco/Euskal Herriko Unibertsitatea for predoctoral fellowships (PIFA01/2007/021). Technical and human support provided by SGIker (UPV/EHU, MICINN, GV/EJ, ESF) is gratefully acknowledged.

---

[1] a) J. J. Perry, J. A. Perman, M. J. Zaworotko, *Chem. Soc. Rev.* **2009**, *38*, 1400–1417; b) G. R. Desiraju, *Angew. Chem. Int. Ed.* **2007**, *46*, 8342–8356; c) D. Braga, L. Brammer, N. R. Champness, *CrystEngComm* **2005**, *7*, 1–19; d) L. Brammer, *Chem. Soc. Rev.* **2004**, *33*, 476–489; e) B. Moulton, M. J. Zaworotko, *Chem. Rev.* **2001**, *101*, 1629–1658; f) D. Braga, F. Grepioni, G. R. Desiraju, *Chem. Rev.* **1998**, *98*, 1375–1405.

[2] a) S. Kitagawa, R. Kitaura, S. Noro, *Angew. Chem. Int. Ed.* **2004**, *43*, 2334–2375; b) K. Biradha, Y. Hongo, M. Fujita, *Angew. Chem. Int. Ed.* **2000**, *39*, 3843–3845; c) H. Li, M. Eddaoudi, M. O'Keeffe, O. M. Yaghi, *Nature* **1999**, *402*, 276–279.

[3] a) G. R. Desiraju, *Acc. Chem. Res.* **2002**, *35*, 565–573; b) C. B. Aakeröy, *Acta Crystallogr., Sect. B* **1997**, *53*, 569–586; c) M. C. T. Fyfe, J. F. Stoddart, *Acc. Chem. Res.* **1997**, *30*, 393–401; d) D. S. Lawrence, T. Jiang, M. Levett, *Chem. Rev.* **1995**, *95*, 2229–2260; e) S. Subramanian, M. J. Zaworotko, *Coord. Chem. Rev.* **1994**, *137*, 357–401.

[4] a) O. M. Yaghi, M. O'Keeffe, N. W. Ockwig, H. K. Chae, M. Eddaoudi, J. Kim, *Nature* **2003**, *423*, 705–714; b) O. R. Evans, W. B. Lin, *Acc. Chem. Res.* **2002**, *35*, 511–522; c) B. J. Holliday, C. A. Mirkin, *Angew. Chem. Int. Ed.* **2001**, *40*, 2022–2043; d) D. Braga, *J. Chem. Soc., Dalton Trans.* **2000**, 3705–3713; e) O. M. Yaghi, H. Li, C. Davis, D. Richardson, T. L. Groy, *Acc. Chem. Res.* **1998**, *31*, 474–484; f) C. Janiak, *Angew. Chem. Int. Ed. Engl.* **1997**, *36*, 1431–1434; g) C. Chen, K. S. Suslick, *Coord. Chem. Rev.* **1993**, *128*, 293–322.

[5] a) E. A. Meyer, R. K. Castellano, F. Diederich, *Angew. Chem. Int. Ed.* **2003**, *42*, 1210–1250; b) M. A. Spackman, J. J. McKinnon, *CrystEngComm* **2002**, 278–392; c) P. Matrangolo, G. Resnati, *Chem. Eur. J.* **2001**, *7*, 2511–2519; d) C. Janiak, *J. Chem. Soc., Dalton Trans.* **2000**, 3885–3896.

[6] a) H. D. Selby, B. K. Roland, M. D. Carducci, Z. Zheng, *Inorg. Chem.* **2003**, *42*, 1556–1662; b) *Metal Clusters in Chemistry* (Eds.: P. Braunstein, L. A. Oro, P. R. Raithby), Wiley-VCH, New York, **1999**.

[7] a) G. Beobide, O. Castillo, U. García-Couceiro, J. P. García-Terán, A. Luque, M. Martínez-Ripoll, P. Román, *Eur. J. Inorg. Chem.* **2005**, 2586–2589; b) C. J. O'Connor, C. L. Klein, R. J. Majeste, L. M. Trefonas, *Inorg. Chem.* **1982**, *21*, 64–67.

[8] a) D. F. Sava, V. Kravtsov, F. Nouar, L. Wojtas, J. F. Eubank, M. Eddaoudi, *J. Am. Chem. Soc.* **2008**, *130*, 3768–3770; b) T. K. Maji, K. Uemura, H.-C. Chang, R. Matsuda, S. Kitagawa, *Angew. Chem. Int. Ed.* **2004**, *43*, 3269–3272; c) D. Li, K. Kaneko, *J. Phys. Chem. B* **2000**, *104*, 8940–8945; d) R. Kitaura, K. Fujimoto, S. Noro, M. Kondo, S. Kitagawa, *Angew. Chem. Int. Ed.* **2002**, *41*, 133–135; e) M. Kondo, T. Okubo, A. Asami, S. I. Noro, T. Yoshitomi, S. Kitagawa, T. Ishii, H. Matsuzaka, K. Seki, *Angew. Chem. Int. Ed.* **1999**, *38*, 140–143.

[9] a) G. Beobide, W.-G. Wang, O. Castillo, A. Luque, P. Román, G. Tagliabue, S. Galli, J. A. R. Navarro, *Inorg. Chem.* **2008**, *47*, 5267–5277; b) G. Beobide, O. Castillo, A. Luque, U. García-Couceiro, J. P. García-Terán, P. Román, *Dalton Trans.* **2007**, 2669–2680.

[10] L. Infantes, S. Motherwell, *CrystEngComm* **2002**, *4*, 454–461.

[11] a) L. Ma, C. Abney, W. Lin, *Chem. Soc. Rev.* **2009**, *38*, 1248–1256; b) A. U. Czaja, N. Trukhan, U. Müller, *Chem. Soc. Rev.* **2009**, *38*, 1284–1293.

[12] a) J. L. Manson, J. Gu, J. A. Schlueter, H. H. Wang, *Inorg. Chem.* **2003**, *42*, 3950–3955; b) T. Ishida, T. Kawakami, S. Mitsubori, T. Nogami, K. Yamaguchiand, H. Iwamura, *J. Chem.*

Soc., Dalton Trans. **2002**, 3177–3186; c) M. Yasui, Y. Ishikawa, N. Akiyama, T. Ishida, T. Nogami, F. Iwasaki, *Acta Crystallogr., Sect. B* **2001**, *57*, 288–295; d) T. Ezuhara, K. Endo, K. Matsuda, Y. Aoyama, *New J. Chem.* **2000**, *24*, 609–613.

[13] a) T. Ishida, S. Mitsubori, T. Nogami, N. Takeda, M. Ishikawa, H. Iwamura, *Inorg. Chem.* **2001**, *40*, 7059–7064; b) F. Mohri, K. Yoshizawa, T. Yamabe, T. Ishida, T. Nogami, *Mol. Eng.* **1999**, *8*, 357–373.

[14] B. Bleaney, K. D. Bowers, *Proc. R. Soc. London, Ser. A* **1952**, *214*, 451–465.

[15] L. K. Thompson, O. Waldmann, X. Zhiqiang, *Coord. Chem. Rev.* **2005**, *249*, 2677–2690.

[16] a) T. Ishida, T. Kawakami, S. I. Mitsubori, T. Nogami, K. Yamaguchi, H. Iwamura, *J. Chem. Soc., Dalton Trans.* **2002**, 3177–3186; b) A. Escuer, R. Vicente, F. A. Mautner, M. A. S. Goher, M. A. M. Abu-Youssef, *Chem. Commun.* **2002**, 64–65; c) F. Lloret, M. Julve, J. Cano, G. De Munno, *Mol. Cryst. Liq. Cryst.* **1999**, *334*, 569–585.

[17] N. Masciocchi, S. Galli, G. Tagliabue, A. Sironi, O. Castillo, A. Luque, G. Beobide, W. Wang, M. A. Romero, E. Barea, J. A. R. Navarro, *Inorg. Chem.* **2009**, *48*, 3087–3094.

[18] R. R. Hunt, J. F. W. McOmie, E. R. Sayer, *J. Chem. Soc.* **1959**, 525–530.

[19] A. Earnshaw, *Introduction to Magnetochemistry*, Academic Press, London, **1968**.

[20] *CrysAlis RED*, version 1.170, Oxford Diffraction, Wroclaw, Poland, **2003**.

[21] A. Altomare, M. C. Burla, M. Camalli, G. L. Cascarano, C. Giacovazzo, A. Guagliardi, A. G. G. Moliterni, R. Spagna, *J. Appl. Crystallogr.* **1999**, *32*, 115–119.

[22] G. M. Sheldrick, *SHELXS97* and *SHELXL97*, University of Göttingen, Germany, **1997**.

[23] L. J. Farrugia, *J. Appl. Crystallogr.* **1999**, *32*, 837–838.

[24] J. Rodríguez-Carvajal, *FULLPROF*, Program for pattern matching analysis of powder patterns. *Abstracts of the Satellite Meeting on Powder Diffraction of the XV Congress of the IUCr*, Toulouse, France, **1990**, 127.

Received: June 29, 2010